nature neuroscience

The idiosyncratic brain: distortion of spontaneous connectivity patterns in autism spectrum disorder

Avital Hahamy[1], Marlene Behrmann[2] & Rafael Malach[1]

Autism spectrum disorder (ASD) has been associated with a reduction in resting state functional connectivity, though this assertion has recently been challenged by reports of increased connectivity in ASD. To address these contradictory findings, we examined both inter- and intrahemispheric functional connectivity in several resting state data sets acquired from adults with high-functioning ASD and matched control participants. Our results reveal areas of both increased and decreased connectivity in multiple ASD groups as compared to control groups. We propose that this heterogeneity stems from a previously unrecognized ASD characteristic: idiosyncratic distortions of the functional connectivity pattern relative to the typical, canonical template. The magnitude of an individual's pattern distortion in homotopic interhemispheric connectivity correlated significantly with behavioral symptoms of ASD. We propose that individualized alterations in functional connectivity organization are a core characteristic of high-functioning ASD, and that this may account for previous discrepant findings.

At rest, the typical adult brain shows activation patterns that are correlated within brain networks. This intra- as well as interhemispheric spontaneous functional connectivity has been robustly demonstrated in studies using functional magnetic resonance imaging (fMRI)[1–3], as well as in human electrophysiological recordings[4,5]. However, close examination reveals that the level of connectivity is not uniform across the cortex: for example, in the case of homotopic interhemispheric connectivity, many primary sensory-motor regions show high levels of connectivity, while higher order association regions do so to a lesser degree[6]. Similarly, intra-network functional connectivity varies between regions comprising each network[7].

A substantial body of research has identified atypicalities in functional connectivity patterns in individuals with ASD, a neurodevelopmental disorder diagnosed on the basis of deficits in social and language abilities, as well as excessive repetitive behaviors[8] (although note that the *Diagnostic and Statistical Manual of Mental Disorders* fifth edition (DSM-V) has different criteria). The atypicalities, which include reduction in various functional connections[9–11], and particularly in interhemispheric connections[12–14], are taken as support for the claim that the ASD brain is characterized by "underconnectivity." However, this claim of underconnectivity has been challenged by recent studies reporting functional overconnectivity in ASD[15–19].

Here we used a large database of fMRI resting state scans (ABIDE)[14] to search for an underlying principle that may reconcile these conflicting findings. Our results reveal a new and robust abnormality in the ASD connectivity, which relates to the topographical nature of the functional connectivity patterns rather than to their overall strength. Specifically, we found that the canonical pattern of functional connectivity seen in typical controls showed significant and individually distinct (idiosyncratic) distortions in participants with ASD. The idiosyncratic nature of these distortions led to high inter-subject variability in the connectivity patterns of individuals with ASD as compared to controls, evident in both intra- and interhemispheric connectivity patterns across all data sets examined. The magnitude of individual distortions in homotopic interhemispheric connectivity was also correlated with behavioral measures of ASD. These findings point to exaggerated variations in the topographies of connection patterns as a possible measure for characterizing brain alterations and symptom severity in ASD, and offer a means for reconciling previous discrepant empirical findings.

RESULTS

Homotopic interhemispheric connectivity

We first analyzed the homotopic interhemispheric functional connections, since they offer a relatively simple yet robust subset of brain connectivity[3,4]. Furthermore, unlike the general case of functional connectivity, the strength of these connections has been consistently demonstrated to be reduced in ASD[12–14]. We examined the voxel-wise differences in homotopic interhemispheric connectivity of adult participants diagnosed with ASD and controls across five separate data sets: CAL (California Institute of Technology), CMU (Carnegie Mellon University), PBG (University of Pittsburgh), Utah-1 (University of Utah, first half) and Utah-2 (University of Utah, second half) (see Online Methods, **Table 1** and **Supplementary Table 1**). To evaluate whether an ASD-related global (average across all connections) underconnectivity of interhemispheric connections was reproducible across all data sets[13], we calculated the ratio between ASD and control groups' global interhemispheric connectivities for each data set (see Online Methods). All ratios were found to be slightly smaller than 1, indicating a weak but consistent reduction in global interhemispheric connectivity in the ASD groups; however, this effect did not survive correction for multiple comparisons (CAL: 0.88, CMU: 0.98, PBG: 0.91, Utah-1: 0.97, Utah-2: 0.94, $\chi^2_{(10)} = 21.22$, $P = 0.48$ corrected, Fisher's method).

[1]Department of Neurobiology, Weizmann Institute of Science, Rehovot, Israel. [2]Department of Psychology, Carnegie Mellon University, Pittsburgh, Pennsylvania, USA. Correspondence should be addressed to R.M. (rafi.malach@gmail.com).

Received 7 May 2014; accepted 10 December 2014; published online 19 January 2015; doi:10.1038/nn.3919

Table 1 Demographics and behavioral statistics for ASD and control groups

	N	Age	Fraction male	Fraction right-handed	FSIQ	VIQ	PIQ	ADOS SOC	ADOS COM	ADOS RRB	ADI SOC	ADI COM	ADI RRB
Control	73	25.82 (0.79)	0.81	0.90	114.01 (1.33)	113.11 (1.41)	111.62 (1.26)						
ASD	68	26.6 (0.77)	0.91	0.93	107.82 (1.92)	105.87 (2)	108.43 (1.83)	8.39 (0.33)	4.8 (0.2)	2.08 (0.22)	20.74 (0.58)	15.85 (0.5)	6.05 (0.3)

Means, with s.e.m. values given in parentheses. FSIQ, full-scale IQ; VIQ, verbal IQ; PIQ, performance IQ; SOC, social; COM, communication; RRB, restricted and repetitive behavior. See also **Supplementary Table 1**.

To assess whether the homotopic interhemispheric underconnectivity of the ASD samples was topographically uniform across the cortex, we inspected group maps of interhemispheric connectivity (see Online Methods). In agreement with previous reports[6], we found a pattern of regional variations of interhemispheric connectivity strengths across the cortex in both control and ASD groups (**Fig. 1a**). The highest interhemispheric connectivity was located in the primary somatosensory and motor cortices (pre- and postcentral gyri), followed by other primary sensory areas (occipital pole, Heschl's gyrus). Areas showing relatively low interhemispheric connectivity were heteromodal association areas, such as the frontal lobe and temporal regions (inferior and middle temporal gyri). However, even qualitative evaluation revealed that there were marked differences between the interhemispheric connectivities of ASD and control groups.

To quantify these interhemispheric connectivity differences between control and ASD groups, we created between-groups *t*-test maps for each data set separately and across the pooled cohort of participants (see Online Methods). These maps revealed both regions of decreased and regions of increased interhemispheric connectivity in ASD participants relative to controls (**Fig. 1c** and **Supplementary Fig. 1**). We also used meta-analysis to assess the consistency in interhemispheric connectivity effects across data sets (see Online Methods). The resulting map displayed both areas of increased and areas of decreased interhemispheric connectivity in ASD groups in comparison to control groups. This map strongly resembled the pooled *t*-test map, confirming the consistency of areas showing either increased or decreased connectivity in ASD participants across data sets (**Supplementary Fig. 2**). Thus, while our results revealed a global underconnectivity trend, they also demonstrated consistent localized instances of overconnectivity in ASD groups as compared to controls.

Spatial structure of group differences

In the search of an underlying principle for the mapping of under- and overconnectivity effects, we compared the between-groups *t*-map with the typical interhemispheric connectivity map in the pooled cohort of participants. Since the mean of each experimental group and the difference between these means as assessed by *t*-tests are mathematically dependent, we compared an averaged interhemispheric connectivity map across all 141 participants with the between-groups difference map (**Fig. 1b**,**c**). These comparisons revealed that the directionality of group differences (control > ASD or ASD > control) in interhemispheric connectivity depended on the typical magnitude of interhemispheric connectivity. Specifically, regions that typically showed high interhemispheric connectivity (for example, sensorimotor cortex, occipital cortex) tended to have reduced connectivity in ASD as compared to control participants. The opposite was true for regions that typically showed low interhemispheric connectivity (for example, frontal cortex, temporal cortex), which tended to have increased interhemispheric connectivity in participants with ASD as compared to controls. We will refer to this phenomenon as a 'regression to the mean' effect.

This 'regression to the mean' effect was also evident in data set–specific analyses. To avoid circularity, we compared between-groups difference maps of each data set with control group maps excluding control participants for which the difference maps were calculated (see Online Methods). These comparisons again revealed that areas of typically high interhemispheric connectivity showed lower levels of connectivity in participants with ASD, and vice versa (**Supplementary Fig. 1**).

A straightforward prediction of the 'regression to the mean' effect is that extreme voxel values (of both high and low interhemispheric connectivity) in the ASD group maps should be attenuated in comparison to voxel values in the control group maps. This would lead to

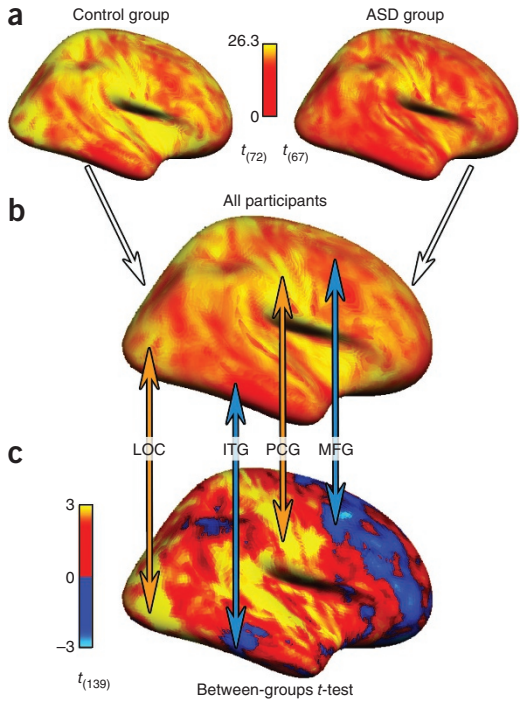

Figure 1 Pooled homotopic interhemispheric group maps and between-groups difference map. (**a**) Control group ($n = 73$) and ASD group ($n = 68$) homotopic interhemispheric maps, combined across all data sets. (**b**) Averaged homotopic interhemispheric map of all control and ASD participants across data sets. (**c**) Pooled between-groups *t*-test map (control > ASD). Arrows demonstrate the correspondence between directionalities of group differences (control > ASD or ASD > control) and regional variation in homotopic interhemispheric connectivity in the brain. The ASD group shows reduced interhemispheric connectivity in regions of typically high interhemispheric connectivity (orange arrows) and increased interhemispheric connectivity in areas of reduced connectivity in the typical brain (blue arrows). Homotopic interhemispheric maps are symmetrical across the midline, so only the right hemisphere is presented. LOC, lateral occipital cortex; ITG, inferior temporal gyrus; PCG, postcentral gyrus; MFG, middle frontal gyrus. See also **Supplementary Figures 1** and **2**, demonstrating the consistency of this effect in each separate data set used in this study.

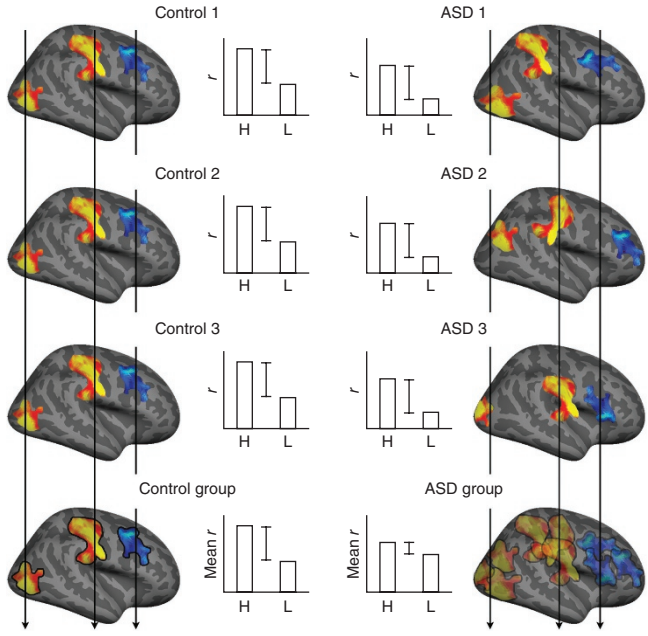

Figure 2 Schematic illustration of the spatial-distortion origins of the 'regression to the mean' effect. Each column presents graphics illustrating three single-subject maps and one group map displaying two areas of high homotopic interhemispheric connectivity (yellow-red) and an area of low interhemispheric connectivity (blue-white). Arrows demonstrate the alignment between single-subject maps. Group maps were created by superimposing single-subject maps. The low spatial variability between maps of control participants (left) results in a group map showing distinct areas of high and low interhemispheric connectivity. However, the idiosyncratic spatial distortions in each ASD single-subject map (right) as compared with the control maps yields a 'regression to the mean' effect in the group map: areas of typically high levels of interhemispheric connectivity show lower connectivity levels, and vice versa. Bars present a quantitative comparison between the two maps of each row. Each bar represents the value of a hypothetical voxel of highest homotopic interhemispheric connectivity (H) and a hypothetical voxel of lowest interhemispheric connectivity (L) of each map. Vertical lines illustrate the dispersion of values in each map. The 'regression to the mean' effect is evident at the group level as lower dispersion of values in the ASD group map as compared to the control group map (bottom). This effect does not stem from the single-subject level, since the dispersions of values within ASD single-subject maps do not differ from those of control maps.

reduced variance of voxel-connectivity values across the ASD group maps as compared to the variance of control group maps. This was indeed found across all data sets, confirming the existence of a consistent 'regression to the mean' effect (CAL: 0.52, CMU: 0.97, PBG: 0.55, Utah-1: 0.37, Utah-2: 0.47, $\chi^2_{(10)} = 30.75$ $P = 0.01$ corrected, Fisher's method).

Origins of the 'regression to the mean' effect

The group-level 'regression to the mean' effect may stem from two different phenomena at the single-subject level. First, the observed group effects may be due to a 'regression to the mean' effect operating within each individual's brain in the ASD group. To test this possibility, we used the same quantitative measure applied to the group maps for the single-subject maps and measured the variance of interhemispheric connectivity values in each individual brain. Comparison of the ratios of group-averaged single-subject variances across data sets did not show a consistent between-groups effect, and most ratios actually showed an opposite trend (higher variance in ASD participants), suggesting that the group 'regression to the mean' effect did not stem from 'regression to the mean' at the single-subject level (CAL: 1.05, CMU: 1.04, PBG: 1.14, Utah-1: 1.1, Utah-2: 0.98).

An alternative explanation for the observed group 'regression to the mean' effect is that participants with ASD showed greater individualistic topographical distortions in their interhemispheric connectivity patterns. To illustrate why such individual distortions should lead to a 'regression to the mean' effect at the group level, we schematically depict this alternative in **Figure 2**. Consistent with the reported findings, under this topographic distortion alternative, mean single-subject variances of interhemispheric connectivity values should not differ between control and ASD-diagnosed participants. By contrast, a misalignment between areas of high or low connectivity magnitudes

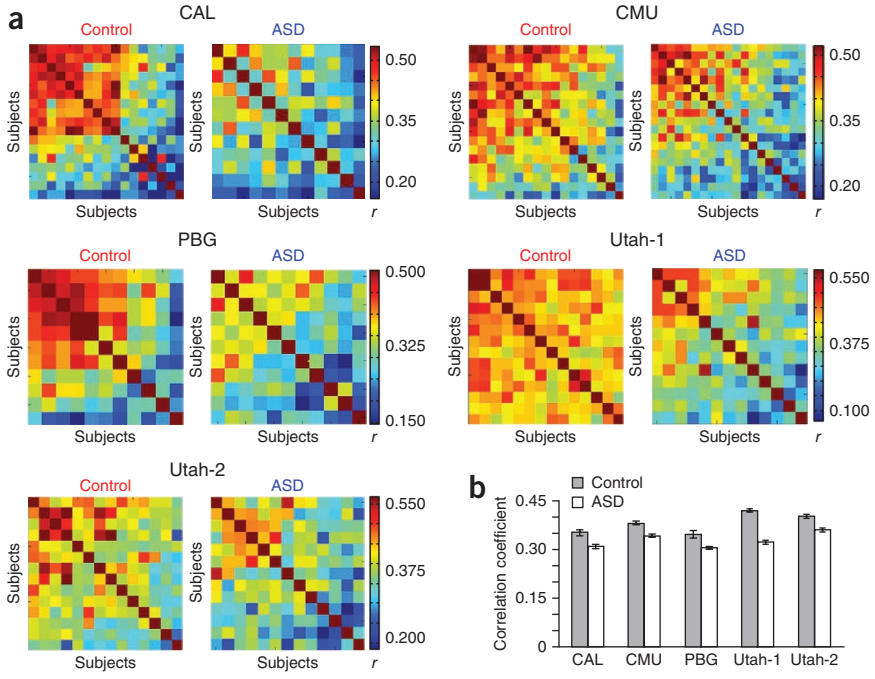

Figure 3 Idiosyncratic distortions of homotopic interhemispheric connectivity patterns in ASD groups. (**a**) For each data set separately, similarity (spatial correlation) matrices are presented for the control group (left) and the ASD group (right). Each row and column presents the similarity between the homotopic interhemispheric connectivity map of a single participant and the maps of all other participants of the same experimental group. Participants in each matrix are ordered by descending mean similarity values. Note the higher levels of inter-subject similarity between participants of the control groups in comparison to those of the ASD groups. (**b**) The mean inter-subject similarity (see Online Methods) of each matrix in **a** is compared between the control and ASD group in each data set. Error bars represent s.e.m. Averaged inter-subject similarities are higher in control than in ASD-diagnosed participants in all data sets, indicating higher levels of idiosyncratic distortions in homotopic interhemispheric connectivity patterns in ASD samples in comparison to the control samples ($\chi^2_{(10)} = 31.95$, $P = 0.01$ corrected, Fisher's method).

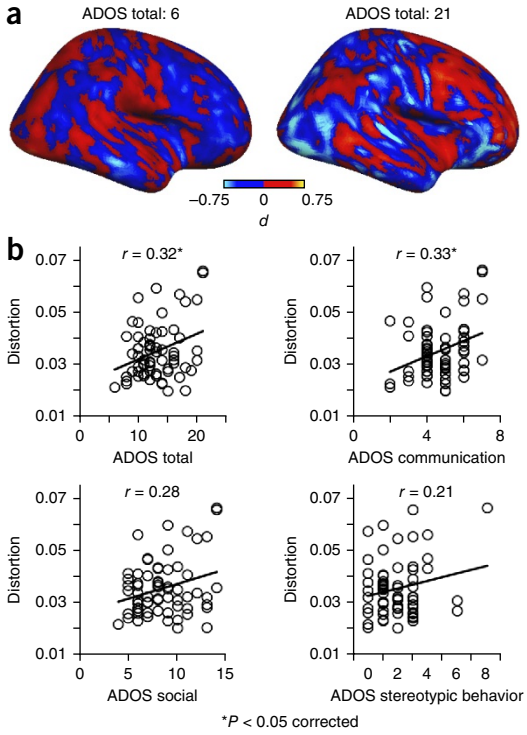

Figure 4 Quantification of individual pattern distortions and correlation with ASD symptoms. (**a**) Subtraction of mean homotopic interhemispheric control values from ASD single-subject values, displayed for two ASD participants of lowest (left) and highest (right) ADOS total score. Note the low variability in homotopic interhemispheric difference values (*d*) in the participant with low ADOS score, indicative of a low level of distortion, and the high variability in interhemispheric difference values in the participant with high ADOS score, indicative of a high level of distortion. The variance of each participant's difference values is referred to as the single-subject distortion index. (**b**) Correlation between single-subject distortion index and ASD symptoms on the ADOS scale. Correlation coefficients are displayed in each panel. Though all correlations were significant before correction for multiple comparisons, only the correlations with ADOS total and ADOS communication (top row) survived correction for multiple comparisons.

across participants with ASD will result in mixing of a range of high and low magnitudes, causing a 'regression to the mean' effect at the group level.

Critically, for this possibility to account for the observed group 'regression to the mean' effect, different ASD participants must show idiosyncratic patterns of interhemispheric connectivity: each individual ASD participant should show a different distortion of the typical pattern. To evaluate this possibility, we computed the spatial correlation between each participant's interhemispheric connectivity pattern and those of all other participants of the same experimental group in each separate data set (see Online Methods). The resulting between-subjects similarity matrices consistently showed higher correlation values (more similarity between interhemispheric connectivity patterns) among control participants than among those with ASD (**Fig. 3a**). The ratios between the overall similarity of connectivity patterns in individuals with ASD as compared to control participants were consistently lower than 1, attesting to a more diverse range of interhemispheric connectivity patterns in participants with ASD as compared to the more reproducible control patterns (CAL: 0.88, CMU: 0.9, PBG: 0.88, Utah-1: 0.77, Utah-2: 0.9, $\chi^2_{(10)} = 31.95$ $P = 0.01$ corrected, Fisher's method; **Fig. 3b**). Thus, our analysis clearly pointed to a wider range of idiosyncratic connectivity patterns in individuals with ASD as the underlying phenomenon that led to the 'regression to the mean' effect in the group interhemispheric connectivity patterns.

Alternatives to the idiosyncrasy of functional patterns

Thus far, we have established that the spatial patterns of interhemispheric connectivity were less similar between ASD participants than between controls. However, it is also possible that there were common pattern distortions in ASD participants across data sets as compared to the canonical control pattern. Such a hypothesis would entail higher correlations among participants with ASD with a canonical ASD pattern (which would contain the systematic pattern distortions) than with a canonical control pattern (which lacks these distortions). However, we did not find such an effect in our data ($t_{(67)} = -0.81$, $P = 0.42$).

While our analysis focused on idiosyncratic patterns in ASD participants, an interesting alternative could be that several distinct patterns exist within the ASD cohort, which may constitute subgroups of individuals with autism. These patterns would be similar across members of the same subgroup but different between subgroups. To evaluate this possibility, we separately submitted homotopic interhemispheric connectivity voxel values of ASD-diagnosed and control participants to *k*-means clustering and tested the resulting clusters using gap statistics[20]. To avoid spurious clustering driven by differences between acquisition sites and protocols, we applied the clustering to each data set separately. Our results revealed that the optimal number of clusters was 1 in both control and ASD samples across data sets. Thus, our analysis did not reveal the existence of a significant difference in clustering among individuals with ASD as compared to controls.

Finally, it is possible that the functional inter-subject variability in ASD may have resulted from anatomical differences. For example, the brains of participants with ASD may show more asymmetry across hemispheres as compared to control brains. However, group differences in the level of anatomical asymmetry were very small and inconsistent across data sets (**Supplementary Table 2**). It is therefore unlikely that this has biased our functional measures.

Relationship to diagnostic tests of ASD

We next hypothesized that the level of connectivity pattern distortion in the brain of each individual with ASD, which underlies the low inter-subject spatial correlations in ASD groups (**Fig. 3**), would be related to behavioral symptoms of ASD. To map the topographical distortions of interhemispheric connectivity for each participant with ASD, we subtracted the control group voxel-wise interhemispheric connectivity values from the corresponding values of each participant with ASD (see Online Methods). The resulting single-subject maps expressed the level of deviation for each voxel from the typical control interhemispheric connectivity pattern. **Figure 4a** presents the voxel deviation maps for the two individuals showing the most extreme Autism Diagnostic Observation Schedule (ADOS) measures (lowest and highest ADOS total scores) in the ASD cohort. As is apparent even on qualitative inspection, the individual with the more severe ASD symptoms showed greater deviations, both positive and negative, from the typical interhemispheric connectivity pattern than the individual with the less severe ASD symptoms. In other words, the variance of deviations from the control pattern was larger in the participant with the more severe symptoms.

We therefore defined a distortion index as the variance of differences in interhemispheric connectivity levels for each individual brain. We found significant positive correlations between the distortion index and all ADOS measures (**Fig. 4b**); however, only the correlations with ADOS total ($r = 0.32$, $P = 0.045$, corrected, $n = 66$)

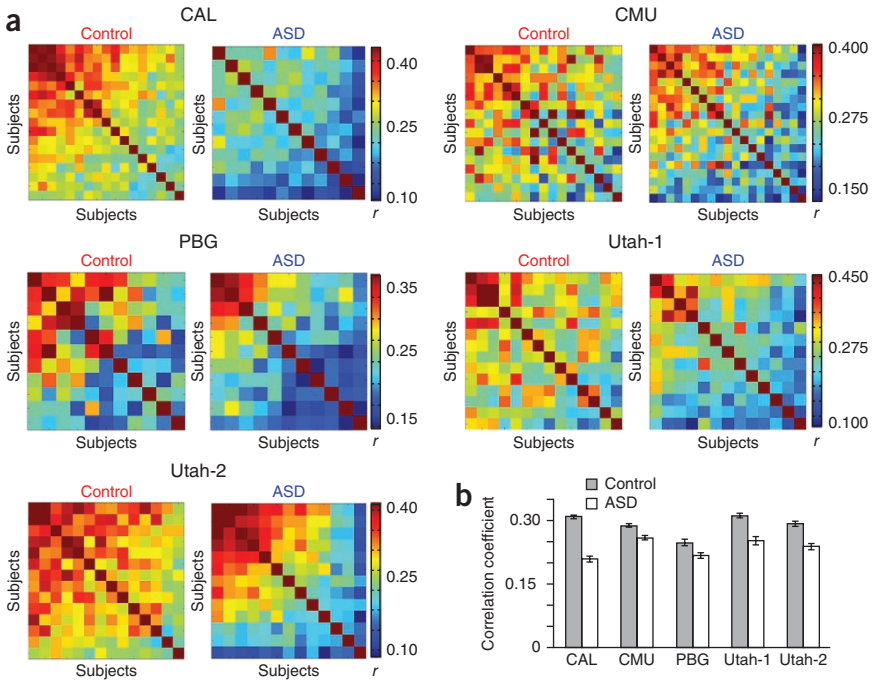

Figure 5 Idiosyncratic distortions of heterotopic interhemispheric connectivity patterns in ASD groups. (**a**) For each data set separately, similarity (spatial correlation) matrices are presented for the control group (left) and the ASD group (right). Each row and column presents the similarity between the heterotopic interhemispheric connectivity values of a single participant and the corresponding values in all other participants of the same experimental group. Participants in each matrix are ordered by descending mean similarity values. Note the higher levels of inter-subject similarity between participants of the control groups in comparison to those of the ASD groups. (**b**) The mean inter-subject similarity (see Online Methods) of each matrix in **a** is compared between the control and ASD group in each data set. Error bars represent s.e.m. Averaged inter-subject similarities are higher in control than in ASD participants in all data sets, indicating higher levels of idiosyncratic distortions in heterotopic interhemispheric connectivity patterns in ASD samples in comparison to the control samples ($\chi^2_{(10)} = 41.28$, $P = 2.4 \times 10^{-4}$ corrected, Fisher's method).

and ADOS communication scores ($r = 0.33$, $P = 0.04$, corrected, $n = 66$) remained significant after applying a Bonferroni correction for multiple comparisons ($P = 0.13$ ADOS social, $P = 0.5$ ADOS stereotypic behavior, corrected). We also computed distortion levels for control participants (see Online Methods). The levels of distortion in control participants were, as expected, below those of ASD participants (ASD/control distortion ratio of 1.13, $P = 0.01$).

Heterotopic interhemispheric and intrahemispheric patterns

Idiosyncratic connectivity distortions may not be unique to homotopic interhemispheric connections but could reflect a more general brain phenomenon. To address this hypothesis, we compared voxel-wise heterotopic interhemispheric connectivity patterns, as well as within-hemisphere connectivity patterns of control and ASD-diagnosed participants (see Online Methods). Extending our finding in the homotopic interhemispheric connectivity patterns, ASD groups showed a consistent reduction in inter-subject spatial similarity (increased idiosyncrasy) in comparison to control groups in the heterotopic interhemispheric connectivity patterns (CAL: 0.68, CMU: 0.9, PBG: 0.88, Utah-1: 0.81, Utah-2: 0.82, $\chi^2_{(10)} = 41.28$ $P = 2.4 \times 10^{-4}$ corrected, Fisher's method; **Fig. 5**). The same phenomenon was evident in connectivity patterns both within the left hemisphere (CAL: 0.74, CMU: 0.9, PBG: 0.89, Utah-1: 0.83, Utah-2: 0.83, $\chi^2_{(10)} = 43.01$

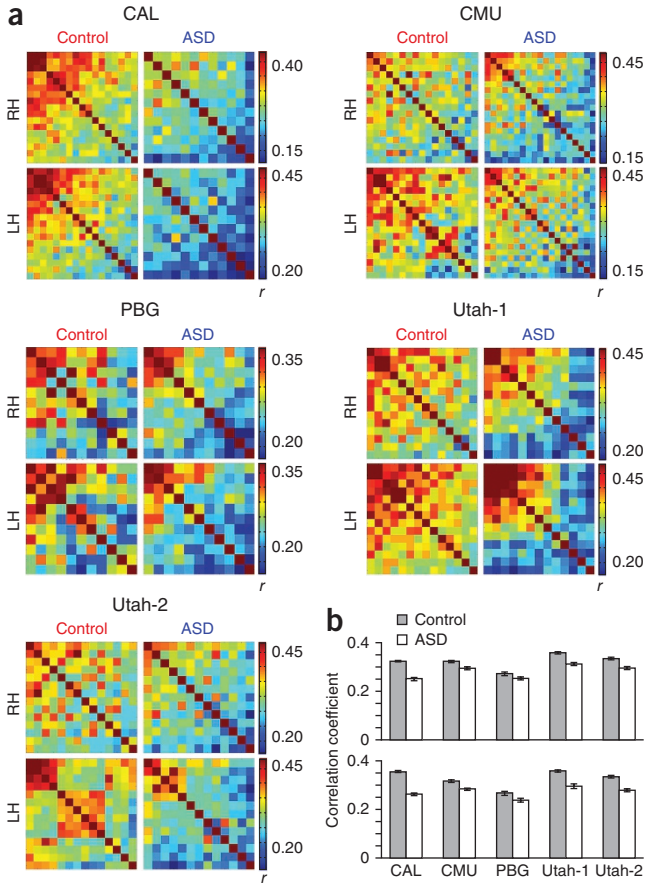

Figure 6 Idiosyncratic distortions of intrahemispheric connectivity patterns in ASD groups. (**a**) For each data set separately, similarity matrices are presented for the control group (left) and the ASD group (right), and for the right hemisphere (top) and left hemisphere (bottom). Within each matrix, each row and column present the similarity between the intrahemispheric connectivity values of a single participant and the corresponding values of all other participants of the same experimental group. Participants in each matrix are ordered by descending mean similarity values. Note the higher levels of intra-subject similarity between participants of the control groups in comparison to those of the ASD groups. (**b**) For each hemisphere separately, the mean intra-subject similarity (see Online Methods) of each matrix in **a** is compared between the control and ASD group in each data set. Error bars represent s.e.m. Averaged intra-subject similarities are higher in control than in ASD participants in all data sets and across hemispheres, indicating higher levels of idiosyncratic distortions in intrahemispheric connectivity patterns in ASD samples in comparison to the control samples (for left and right hemispheres, respectively, $\chi^2_{(10)} = 43.01$, $P = 1.2 \times 10^{-4}$ corrected; $\chi^2_{(10)} = 34.47$, $P = 0.004$ corrected; Fisher's method).

$P = 1.2 \times 10^{-4}$ corrected, Fisher's method; **Fig. 6**) and within the right hemisphere (CAL: 0.77, CMU: 0.91, PBG: 0.93, Utah-1: 0.87, Utah-2: 0.88, $\chi^2_{(10)} = 34.47$ $P = 0.004$ corrected, Fisher's method; **Fig. 6**).

We next calculated single-subject distortion indices for heterotopic interhemispheric patterns and for the patterns within each hemisphere (see Online Methods) and correlated these indices with clinical ASD measures, age and IQ scores. Although significant positive correlations were found between ADOS measures and the distortion indices of both heterotopic connections and the right hemisphere's connections, these correlations did not survive correction for multiple comparisons (corrected *P* values for heterotopic interhemispheric connectivity: ADOS total, 0.25; ADOS social, 0.2; corrected *P* values for right hemisphere connectivity: ADOS total, 0.17; ADOS social 0.12).

If underconnectivity is a global characteristic of the ASD brain[9,11], then all brain connections should demonstrate lower amplitudes in ASD as compared to control groups. However, unlike in the homotopic interhemispheric connectivity case, our analyses failed to reveal a consistent global underconnectivity effect either in the heterotopic interhemispheric connections (CAL: 0.72, CMU: 1.08, PBG: 0.85, Utah-1: 1.15, Utah-2: 1.04), in the left hemisphere connections (CAL: 0.72, CMU: 1.08, PBG: 0.87, Utah-1: 1.13, Utah-2: 1.02) or in the right hemisphere connections (CAL: 0.74, CMU: 1.08, PBG: 0.84, Utah-1: 1.15, Utah-2: 1.06).

For additional analyses, see **Supplementary Tables 3–5** for intrahemispheric connectivity as a function of distance, **Supplementary Tables 6** and **7** for group comparisons of head-motion and brain alignment and **Supplementary Table 8** for IQ-related analyses. **Supplementary Table 9** summarizes our main findings using the statistics described above and additional procedures.

DISCUSSION

Spatially distorted connectivity patterns in ASD

Our study reveals a new characteristic of brain abnormality in adults with high-functioning ASD. We found that the topographic pattern of resting state functional connectivity in ASD participants was significantly distorted relative to the more consistent pattern found across typical participants. These distortions were idiosyncratic in that individual ASD participants tended to differ from each other in their functional connectivity patterns to a greater degree than was true for the control participants.

The most direct evidence for the topographical distortion phenomenon was the significantly lower inter-subject similarity of the functional connectivity spatial patterns across ASD individuals as compared to control participants. We consistently found this effect in different connectivity types: in the patterns of functional connectivity within each hemisphere (**Fig. 6**) as well as in the functional connectivity between the hemispheres (**Figs. 3** and **5**).

The increased spatial diversity led to the observation of a 'regression to the mean' effect as a result of reduced variance in the ASD group maps of homotopic interhemispheric connectivity. It is important to note that a 'regression to the mean' effect at the group level could also result from possible misalignment of homotopic voxels across the two hemispheres in individual brains of participants with ASD. However, such misalignments would necessarily result in attenuation of extreme interhemispheric connectivity values ('regression to the mean') at the single-subject level, which was not the case.

It is also possible that at least part of the increased variability among individuals with ASD resulted from the existence of distinct ASD subtypes (subgroups of participants with ASD whose patterns were more correlated to each other than to those of individuals with other subtypes of ASD). While we failed to find subgroups in the homotopic interhemispheric connectivity patterns, these results cannot be taken as evidence against the possibility of ASD subtypes. The space of possible connectivity patterns is vast, and it is possible that far larger data sets must be analyzed to uncover such clustering. It is also possible that larger cohorts of participants would have revealed consistent pattern distortions across data sets, though our results did not reveal such an effect.

Relation to behavioral measures

Previous studies have framed connectivity changes in ASD as a categorical trait (which differentiates autistic from non-autistic individuals), while other neurophysiological parameters have been framed as dimensional traits (placing ASD at the end of a continuous spectrum with controls)[21]. Our results appear to be compatible with both categorical and dimensional aspects, since the idiosyncratic functional patterns categorically differentiated between individuals with and without autism, but the level of idiosyncrasy corresponded with the level of autism severity on the ADOS scale (**Fig. 4b**). Further neural and behavioral comparisons of individuals with ASD, their relatives and control participants are needed to assess whether the reported functional idiosyncrasy in ASD may be an extreme end of dimensionally distributed functional patterns in the general population.

Unlike the ADOS scores, which reflect ASD symptoms in adulthood[22], Autism Diagnostic Interview (ADI) scores (which reflect childhood history)[23] did not correlate with the level of idiosyncratic distortion. However, since ADI scores were only available for roughly half of the participants across the ASD groups, it is not currently possible to determine whether our reported effects may have developmental origins, or might be related to compensatory mechanisms. Taken together with the absence of a relation between idiosyncratic distortions and age in our current samples of adults, further studies on children with ASD are needed to address the developmental aspects of our findings.

The relationship between behavioral measures and heterotopic interhemispheric as well as intrahemispheric spatial distortions revealed only a nonsignificant trend, albeit in the same direction as the homotopic interhemispheric findings. This may suggest that distortions in homotopic interhemispheric connectivity patterns are a more sensitive marker for ASD, possibly owing to higher signal-to-noise ratio in comparison to other subsets of brain connections[4]. We also note that the significance of correlations between idiosyncratic patterns and behavioral symptoms were weaker than those of our other reported effects. As behavioral measures of ASD are notoriously difficult to quantify, the source of the variability in these correlations remains to be clarified.

It is also important to stress that we did not find significant correlations between the levels of distortion and IQ scores. The absence of correlations with IQ indicates that, although there was a significant IQ difference between experimental groups in some of the analyzed data sets, this IQ difference was unlikely to be the source of the distortion differences between groups.

Relation to previous functional connectivity findings

Our group results failed to reveal significant global underconnectivity effects across different types of brain connections[9–11]. However, our results demonstrated that both increased and decreased connectivity in ASD groups in comparison to control groups may be contributed by spatial distortions in connectivity patterns at the individual level. In the homotopic interhemispheric connectivity case, averaging such distorted patterns across individuals led to the apparent 'dilution' of high and low connectivity strengths, reflected in a 'regression to the

mean' effect in the ASD group maps. Thus, our findings suggest that caution should be exercised when interpreting regional group differences between controls and individuals with ASD, as these may also be related to ASD idiosyncratic connectivity patterns.

The use of multi-site data

The finding of idiosyncratic spatial distortions in connectivity across all analyzed ASD samples attests to the robustness of this effect, particularly when considering the variability of data sets included in this study (see **Supplementary Table 10**). Although we could not control for experiment-related sources of variability (for example, different experimental protocols), the spatial distortions in connectivity patterns were sufficiently pronounced to over-ride any methodological or demographic differences between data sets.

Moreover, the fact that we were able to characterize functional connectivity in a large sample of individuals, whose data were acquired at different sites, allowed us to control for other sources of variability that might explain previously inconsistent neuroimaging findings. First, we limited variability in the demographic and clinical characteristics of the participants with ASD by restricting our analyses to adults with high-functioning ASD[24]. Second, we used the same data processing methodology for all data sets[17]. Third, we carefully controlled for non-neuronal contributions to the fMRI signal by applying methods that reduce the influence of head movements on functional data[25].

Possible sources of the idiosyncratic functional patterns

What mechanism might give rise to the idiosyncrasy of spontaneous connectivity patterns in ASD? When considering distortions of homotopic interhemispheric functional connectivity patterns, a straightforward possibility is that alterations in hemispheric structural laterality exist in ASD. However, between-groups comparisons of structural laterality did not support this possibility (**Supplementary Table 2**). Another possibility might be that individuals with ASD have atypically shaped brains[26]. In such a case, the transformation to standard space could cause altered anatomies to drive the observed functional idiosyncrasy. However, we did not find group differences in the level of distortion caused by the transformation to standard space (**Supplementary Table 7**), arguing against this alternative.

A further possibility is that group differences might be related to idiosyncratic differences in task-related neural activity. Some findings that are compatible with this possibility have been reported in adults and adolescents diagnosed with high-functioning ASD. Specifically, both intra- and interhemispheric idiosyncratic activations have been documented during a simple motor task[27], more complex visuomotor learning[28], face processing[29,30] and naturalistic sensory stimulation[31]. While these studies mostly examined the activity of specific brain regions under well-defined tasks and using relatively small sample sizes, our results offer a general framework within which previous findings may be interpreted. Namely, the presence of idiosyncratic functional connectivity patterns across all brain regions and connection types, even in the absence of an external task, and across a large cohort of participants, proposes functional idiosyncrasy as a new neural characteristic of ASD.

In addition, the emergence of this idiosyncrasy in the absence of an external task is of great interest, since spontaneously emerging functional connectivity patterns have recently been shown to be shaped by the routine behavior of individuals over the course of daily life[32]. As previously postulated, habitual behaviors driven by interactions with the external environmental may be encoded as synaptic efficacies and may emerge in the absence of overt behavior, during rest[33,34]. By extension, it is tempting to conjecture that the idiosyncratic connectivity patterns of individuals with ASD may similarly stem from the altered interaction of the autistic individual with the external environment. Under the assumption that social and physical environmental factors and the brain activations they elicit are largely shared across typical individuals, the environment-neural interactivity will act to regularize network organizations, leading to convergence into a canonical, typical brain. In contrast, the behavioral disconnection of individuals diagnosed with ASD from such regularizing interactions, in addition to their well-documented unreliable and hyper-plastic responses to the external environment[35,36], may result in an aberrant and idiosyncratic connectivity pattern in the brain of each individual with ASD. An interesting question for future studies is whether such connectivity idiosyncrasies may emerge in other clinical populations exhibiting abnormal brain–environment interactivity.

METHODS

Methods and any associated references are available in the online version of the paper.

Note: Any Supplementary Information and Source Data files are available in the online version of the paper.

ACKNOWLEDGMENTS

The authors would like to thank H. Dubossarsky and T. Golan for numerous discussions and suggestions that contributed greatly to this work, and Y. Cohen for assistance with illustrations. This study was supported by the Israeli Presidential Bursary for outstanding PhD students in brain research (A.H.); the Simons Foundation SFARI award 298640 and the Pennsylvania Department of Health SAP grant 4100047862 (M.B.); and a European Union Future Emerging Technologies -7 – Virtual Embodiment and Robotic Re-Embodiment, Israeli Science Foundation, and Israeli Center of Research Excellence grant 51/11, European Union Flagship The Human Brain Project and the Helen and Martin Kimmel award (R.M.). Funding sources for the ABIDE data sets are listed at http://fcon_1000.projects.nitrc.org/indi/abide/index.html.

AUTHOR CONTRIBUTIONS

A.H. conducted the data analyses; A.H., M.B. and R.M. interpreted the results and wrote the manuscript; R.M. supervised the project.

COMPETING FINANCIAL INTERESTS

The authors declare no competing financial interests.

1. Biswal, B., Yetkin, F.Z., Haughton, V.M. & Hyde, J.S. Functional connectivity in the motor cortex of resting human brain using echo-planar MRI. *Magn. Reson. Med.* **34**, 537–541 (1995).
2. Raichle, M.E. *et al.* A default mode of brain function. *Proc. Natl. Acad. Sci. USA* **98**, 676–682 (2001).
3. Salvador, R. *et al.* Neurophysiological architecture of functional magnetic resonance images of human brain. *Cereb. Cortex* **15**, 1332–1342 (2005).
4. Nir, Y. *et al.* Interhemispheric correlations of slow spontaneous neuronal fluctuations revealed in human sensory cortex. *Nat. Neurosci.* **11**, 1100–1108 (2008).
5. He, B.J., Snyder, A.Z., Zempel, J.M., Smyth, M.D. & Raichle, M.E. Electrophysiological correlates of the brain's intrinsic large-scale functional architecture. *Proc. Natl. Acad. Sci. USA* **105**, 16039–16044 (2008).
6. Stark, D.E. *et al.* Regional variation in interhemispheric coordination of intrinsic hemodynamic fluctuations. *J. Neurosci.* **28**, 13754–13764 (2008).
7. Buckner, R.L., Andrews-Hanna, J.R. & Schacter, D.L. The brain's default network: anatomy, function, and relevance to disease. *Ann. NY Acad. Sci.* **1124**, 1–38 (2008).
8. American Psychiatric Association. *DSM-IV-TR: Diagnostic and Statistical Manual of Mental Disorders* (American Psychiatric Press, Washington, DC, 2000).
9. Just, M.A., Cherkassky, V.L., Keller, T.A. & Minshew, N.J. Cortical activation and synchronization during sentence comprehension in high-functioning autism: evidence of underconnectivity. *Brain* **127**, 1811–1821 (2004).
10. Belmonte, M.K. *et al.* Autism and abnormal development of brain connectivity. *J. Neurosci.* **24**, 9228–9231 (2004).
11. Schipul, S.E., Keller, T.A. & Just, M.A. Inter-regional brain communication and its disturbance in autism. *Front. Syst. Neurosci.* **5**, 10 (2011).
12. Dinstein, I. *et al.* Disrupted neural synchronization in toddlers with autism. *Neuron* **70**, 1218–1225 (2011).
13. Anderson, J.S. *et al.* Decreased interhemispheric functional connectivity in autism. *Cereb. Cortex* **21**, 1134–1146 (2011).

14. Di Martino, A. *et al.* The autism brain imaging data exchange: towards a large-scale evaluation of the intrinsic brain architecture in autism. *Mol. Psychiatry* **19**, 659–667 (2014).
15. Keown, C.L. *et al.* Local functional overconnectivity in posterior brain regions is associated with symptom severity in autism spectrum disorders. *Cell Reports* **5**, 567–572 (2013).
16. Supekar, K. *et al.* Brain hyperconnectivity in children with autism and its links to social deficits. *Cell Reports* **5**, 738–747 (2013).
17. Müller, R.A. *et al.* Underconnected, but how? A survey of functional connectivity MRI studies in autism spectrum disorders. *Cereb. Cortex* **21**, 2233–2243 (2011).
18. Uddin, L.Q. *et al.* Salience network-based classification and prediction of symptom severity in children with autism. *JAMA Psychiatry* **70**, 869–879 (2013).
19. Lynch, C.J. *et al.* Default mode network in childhood autism: posteromedial cortex heterogeneity and relationship with social deficits. *Biol. Psychiatry* **74**, 212–219 (2013).
20. Tibshirani, R., Walther, G. & Hastie, T. Estimating the number of clusters in a data set via the gap statistic. *J. R. Stat. Soc. Series B Stat. Methodol.* **63**, 411–423 (2001).
21. Belmonte, M.K., Gomot, M. & Baron-Cohen, S. Visual attention in autism families: 'unaffected' sibs share atypical frontal activation. *J. Child Psychol. Psychiatry* **51**, 259–276 (2010).
22. Lord, C. *et al.* The autism diagnostic observation schedule-generic: a standard measure of social and communication deficits associated with the spectrum of autism. *J. Autism Dev. Disord.* **30**, 205–223 (2000).
23. Lord, C., Rutter, M. & Le Couteur, A. Autism Diagnostic Interview—Revised: a revised version of a diagnostic interview for caregivers of individuals with possible pervasive developmental disorders. *J. Autism Dev. Disord.* **24**, 659–685 (1994).
24. Anagnostou, E. & Taylor, M.J. Review of neuroimaging in autism spectrum disorders: what have we learned and where we go from here. *Mol. Autism* **2**, 4 (2011).
25. Tyszka, J.M., Kennedy, D.P., Paul, L.K. & Adolphs, R. Largely typical patterns of resting-state functional connectivity in high-functioning adults with autism. *Cereb. Cortex* **24**, 1894–1905 (2014).
26. Carper, R.A. & Courchesne, E. Localized enlargement of the frontal cortex in early autism. *Biol. Psychiatry* **57**, 126–133 (2005).
27. Müller, R.A., Pierce, K., Ambrose, J.B., Allen, G. & Courchesne, E. Atypical patterns of cerebral motor activation in autism: a functional magnetic resonance study. *Biol. Psychiatry* **49**, 665–676 (2001).
28. Müller, R.A., Kleinhans, N., Kemmotsu, N., Pierce, K. & Courchesne, E. Abnormal variability and distribution of functional maps in autism: an FMRI study of visuomotor learning. *Am. J. Psychiatry* **160**, 1847–1862 (2003).
29. Scherf, K.S., Luna, B., Minshew, N. & Behrmann, M. Location, location, location: alterations in the functional topography of face- but not object- or place-related cortex in adolescents with autism. *Front. Hum. Neurosci.* **4**, 26 (2010).
30. Pierce, K., Muller, R.A., Ambrose, J., Allen, G. & Courchesne, E. Face processing occurs outside the fusiform 'face area' in autism: evidence from functional MRI. *Brain* **124**, 2059–2073 (2001).
31. Hasson, U. *et al.* Shared and idiosyncratic cortical activation patterns in autism revealed under continuous real-life viewing conditions. *Autism Res.* **2**, 220–231 (2009).
32. Hahamy, A. *et al.* Normalisation of brain connectivity through compensatory behaviour, despite congenital hand absence. *eLife* **4**, e4605 (2015).
33. Harmelech, T. & Malach, R. Neurocognitive biases and the patterns of spontaneous correlations in the human cortex. *Trends Cogn. Sci.* **17**, 606–615 (2013).
34. Sadaghiani, S. & Kleinschmidt, A. Functional interactions between intrinsic brain activity and behavior. *Neuroimage* **80**, 379–386 (2013).
35. Dinstein, I. *et al.* Unreliable evoked responses in autism. *Neuron* **75**, 981–991 (2012).
36. Markram, H., Rinaldi, T. & Markram, K. The intense world syndrome–an alternative hypothesis for autism. *Front Neurosci* **1**, 77–96 (2007).

ONLINE METHODS

Participants. The resting state and structural imaging data of 68 participants with ASD (mean age 26.6, age range 18–42, 62 males) and 73 control participants (mean age 25.82, age range 18–44, 59 males) aggregated from multiple sites[14] were analyzed in this study. No blinding was done. Inclusion criteria for sites were a total of at least 10 ASD participants who met the inclusion criteria for participants and had successful preprocessing as described below. Included data sets were from the Carnegie Mellon University (CMU), the California Institute of Technology (CAL), the School of Medicine at the University of Utah (Utah) and the University of Pittsburgh (PBG). Data from additional participants not available online (4 controls, 5 ASD) were added to the CMU data set. The Utah data set, which was much larger than all other data sets, was randomly split, such that each subsample included 14 control participants and 13 with ASD. Thus, we created five independent data sets of relatively similar sizes for all following comparisons.

Inclusion criteria for ASD participants were a diagnosis of high-functioning ASD on the basis of the ADOS-G[22] and/or ADI-R[23]. ASD and control participants were excluded if they were below the age of 18 or above the age of 45, and if they had large (>1.5 mm) head movements during the scan. **Table 1** summarizes the demographics and behavioral statistics for the entire cohort of participants, and **Supplementary Table 1** describes the ASD and control groups in each data set separately. **Supplementary Table 10** presents details regarding the experimental design used to acquire each data set. Details of acquisition, informed consent, site-specific protocols, specific diagnostic criteria and medication usage at the time of the scan for each data set can be found at http://fcon_1000.projects.nitrc.org/indi/abide/index.html. The following committees approved the protocols of each site: the Human Subjects Protection Committee of the California Institute of Technology (CAL), the Institutional Review Board at Carnegie Mellon University (CMU), the Institutional Review Board at the University of Pittsburgh (PBG) and the University of Utah Institutional Review Board (Utah). Though the medication profiles vary across participants and data sets, the consistency of results across data sets suggests that the findings are not driven by specific medication regimens.

fMRI data analysis. All fMRI data were processed using FSL 5.0.2.1 (http://www.fmrib.ox.ac.uk/fsl/) and in-house Matlab code (MathWorks, Natick, MA, USA). Functional data were analyzed using FMRIB's expert analysis tool (FEAT, version 6). The following preprocessing was applied to the data of each individual participant: motion correction using MCFLIRT[37], brain extraction using BET[38] and high-pass temporal filtering with a cut-off frequency of 0.01 Hz. Functional images were aligned with high-resolution anatomical volumes initially using linear registration (FLIRT), then optimized using boundary-based registration[39]. Structural images were transformed to standard MNI space using a nonlinear registration tool (FNIRT), and the resulting warp fields were applied to the functional images. Normalized files were manually inspected to verify that the transformation was successful. Tissue-type segmentation was carried out using FAST[40], and ventricles and white-matter masks were drawn, avoiding the boundaries between tissue types. The motion parameters of each participant were inspected to identify severe head movements. Head movements of 1–1.5 mm that appeared at either the beginning or end of the scanning session were cropped from the relevant files. Data from participants whose head motion exceeded 1.5 mm were removed from subsequent analyses. Small head movements that might affect the BOLD signal were identified using a scrubbing procedure[41]. Functional data were low-pass filtered with a cutoff frequency of 0.1 Hz, and motion parameters from the six axes of head movements were band-pass filtered (0.01–0.1 Hz)[42]. The non-neuronal contributions to the BOLD signal were removed by linear regression of motion parameters and ventricle and white-matter time courses for each participant[43], all confined to a relevant temporal mask[41]. Global signal regression was not performed, as this procedure has been shown to bias group comparisons[44,45]. The data were then spatially smoothed using a Gaussian filter of 8 mm full width at half maximum.

Interhemispheric connectivity. A voxel-wise method for analyzing homotopic interhemispheric connectivity patterns was employed[12,13]. For each subject separately, the time course of each voxel was correlated with the time course of the homologous voxel in the other hemisphere (as determined by the *x* coordinates in MNI space). Note that possible voxel-wise anatomical asymmetries between the two hemispheres were accounted for by applying spatial-smoothing with a relatively wide Gaussian kernel, as previously described[12]. However, this large smoothing may cause the mixing of BOLD signals from the two cerebral hemispheres along the midline area, thus precluding our ability to test the separate contribution of the medial aspects of each hemisphere to the interhemispheric connectivity. We therefore restricted all further voxel-wise interhemispheric analyses to the lateral aspects of the brain by including only gray-matter voxels that were at least 8 mm away from the midline. Also, note that the homotopic interhemispheric analysis necessarily creates symmetrical maps. Thus it is sufficient to conduct all further analyses on data of a single hemisphere.

Group comparison of global interhemispheric connectivity. To test whether the overall (global) level of interhemispheric connectivity in the single-subject level was reduced in ASD participants as compared to controls[13], the average of each participant's interhemispheric connectivity voxel values was calculated. In each data set separately, these mean interhemispheric connectivity values of all participants from the same experimental group (control or ASD) were averaged, and the ratio between the ASD and control group averages was calculated.

Next, the consistency in directionalities of global interhemispheric connectivity effects across all data sets was assessed using a stringent criterion. Specifically, a global underconnectivity effect in the ASD samples (ASD/control < 1) would be defined as consistent if ratios smaller than 1 were to be observed across all data sets (the probability of obtaining a ratio smaller than 1 across all five data sets is $1/2^5$, $P < 0.05$). Here, and in all further similar analyses, uniform directionalities across all data set–specific effects were taken to indicate a consistent trend, which allowed further testing to assess its magnitude.

To assess the magnitude of these global underconnectivity effects, data set–specific *P* values were calculated using randomization tests, under the null hypothesis of no group differences in the levels of global interhemispheric connectivity. Specifically, within each data set separately, participants' labels (ASD or control) were permuted, creating two random experimental groups, and the between-groups ratio of global interhemispheric connectivity was calculated as explained above (ASD/control). This procedure was repeated 10,000 times, creating 10,000 random ratios that constructed the null distribution, from which the one-sided data set–specific *P* value was obtained. All resulting data set–specific *P* values were then tested using Fisher's method[46,47]. Here, and in all similar analyses, significant *P* values were corrected for multiple hypotheses testing using the highly conservative Bonferroni correction. To establish the robustness of the reported effects, *P* values were additionally tested using Stouffer's test[48] and the weighted *Z*-test with weights set to the square root of each sample size[49] (see **Supplementary Tables 5** and **9**).

Data set–specific group maps and between-groups difference maps. To examine regional variations in interhemispheric connectivity differences between experimental groups, correlation coefficients of each participant's voxels were converted to *z* values using Fisher's *r*-to-*z* transformation to improve normality. For each data set separately, voxelwise group and between-groups two-tailed *t*-tests were run using a general linear model (GLM) design, including group as a factor. For data sets that showed a significant IQ difference between experimental groups (CAL, one subgroup of Utah), the relevant IQ variables were also added as nuisance regressors to the GLM designs. For presentation purposes, resulting unthresholded group and between-groups *t*-values were projected onto an inflated MNI template brain using FreeSurfer (http://surfer.nmr.mgh.harvard.edu/). Note that these maps are presented without any statistical threshold, as they are used for whole-brain topographic pattern comparisons rather than for standard statistical inference, as will be described below. Therefore, correction for multiple comparisons is not applied to these maps.

Pooled analysis and meta-analysis. Pooled interhemispheric connectivity group (control or ASD) and between-groups two-tailed *t*-test maps were created using a GLM design including group as a factor, and acquisition site and IQ scores as nuisance variables[50]. An additional pooled interhemispheric connectivity map of all participants, independent of diagnosis, was created by averaging the two pooled group maps, thus accounting for the different numbers of subjects in the two pooled experimental groups. To verify that the between-groups *t*-test was not biased as a result of the different numbers of participants in the different data sets, we compared the pooled analysis to a meta-analysis of these data. First, the interhemispheric between-groups *t*-test maps of each separate data set

doi:10.1038/nn.3919

were converted to Hedges's *g*-effect size maps[51]. Then a weighted mean of effect sizes across data sets, along with a confidence interval, were calculated for each voxel[52,53]. For presentation purposes, resulting unthresholded statistical values were projected onto an inflated MNI template brain using FreeSurfer.

Assessment of the spatial structure of group differences. We next set out to examine the relationship between the directionality of the interhemispheric differences between groups (control > ASD or ASD > control) and the magnitude of interhemispheric connectivity in the typical brain. 'Regression to the mean' of interhemispheric connectivity values in the ASD groups in comparison to the control groups would be established if a reduction in interhemispheric connectivity would be evident in ASD groups in areas of typically high interhemispheric connectivity, and an increase in interhemispheric connectivity would be evident in ASD groups in areas of typically low connectivity. This relation can be assessed by qualitatively comparing the between-groups interhemispheric *t*-test maps with the interhemispheric maps of the control groups. However, group differences and group means are mathematically dependent. To create an unbiased estimate, we differentiated the data used in the between-groups *t*-test from the data used to calculate the control group *t*-values. Specifically, for the pooled cohort, we compared the between-groups interhemispheric *t*-test map with the average of the two pooled group maps, since differences of means and sum of means are not correlated. For the data set–specific comparisons, for each data set k we define A_k = ASD group, C_k = control group. Each data set–specific between-groups difference map (C_k versus A_k) was compared to a control group map comprising data pooled across all other data sets ($\{C_1, \ldots C_5\} - \{C_k\}$), thus omitting from the reference data those controls who had formed one side of the within-data set difference map. These aggregated control group maps were created using a GLM design including acquisition sites as nuisance variables, thus removing the variance in the data explained by differences between acquisition sites[50].

A quantitative measure for the 'regression to the mean' effect at the group level was also obtained by comparing the variance of interhemispheric connectivity voxel values between the ASD and control group maps of each data set. High variance would indicate the existence of areas of both very high and very low interhemispheric connectivity, whereas low variance would indicate the presence of more midscale connectivity values across the brain. Specifically, for each data set separately, the cross-voxel variance in interhemispheric connectivity was computed for the control and ASD group maps, and the ratio between ASD group variance and control group variance was derived. This procedure resulted in five data set–specific group variance ratios. A consistent 'regression to the mean' effect of the interhemispheric connectivity values in the ASD groups was defined as ratios being lower than 1 across all five data sets (uniform directionalities of effects across all data sets). Effect magnitudes were assessed using randomization tests, under the null hypothesis of no difference in voxel-wise variance between experimental group maps. Specifically, participants' labels were permuted within each separate data set, creating two random experimental groups. Two group *t*-maps were then created using a GLM design including group as a factor and IQ variables as nuisance regressors, and the ratio between voxel-wise variances of the two group maps was calculated. This procedure was repeated 10,000 times, creating the null distribution, which was used in the same statistical procedure as described above.

Subject-level variance comparison. To assess whether the 'regression to the mean' effect was evident at the single-subject level, the interhemispheric connectivity variance across voxels was calculated for each participant. In each data set separately, these single-subject variances were averaged across participants of each experimental group, and the ratio between mean ASD variance and mean control variance was derived. This procedure resulted in five data set–specific variance ratios, and the uniformity of their directionalities was assessed. As no consistent effect was found, integration of data set–specific *P* values was not performed.

Inter-subject spatial correlation of homotopic interhemispheric values. To examine ASD idiosyncrasy in homotopic interhemispheric connectivity patterns, similarity matrices were created for each experimental group. For each data set separately, spatial correlations were computed between the interhemispheric functional connectivity voxel values of each participant and the corresponding values in each other participant of the same experimental group. This resulted in a correlation matrix in which every entry represented the level of similarity between the interhemispheric patterns of each pair of participants (the correlation coefficient for each pair of participants appears twice in such a matrix). The lower triangular entries of this matrix, which contain only one correlation coefficient for each pair of participants, were averaged for each experimental group in each data set, and the ratio between ASD and control averaged values was derived. The uniformity of directionalities of the five resulting ratios (obtained from the five separate ASD and control groups) was assessed. Effect magnitudes were determined using randomization tests, under the null hypothesis of no difference in inter-subject spatial correlation between experimental groups, and used in the same statistical procedure as described above.

Alternatives to the idiosyncrasy of functional pattern. The existence of possible systematic patterns of distortions was evaluated across ASD participants. To this end, homotopic interhemispheric connectivity voxel values of each participant with ASD were correlated with two sets of corresponding voxel values: values averaged across the pooled control participants, and values averaged across the pooled ASD participants, excluding the participant for which the correlations were computed. The resulting two correlation coefficients created for each participant with ASD were Fisher-transformed and compared across participants using a two-tailed paired sample *t*-test.

To assess whether participants with ASD may be divided into subgroups on the basis of similarity in their distortion patterns, *k*-means clustering and gap statistics[20] were employed as implemented in Matlab statistics toolbox (evalclusters). In each data set, the interhemispheric spatial patterns of ASD and control participants underwent separate *k*-means clustering procedures, iteratively using 1–4 clusters. In each such iteration, the within-cluster sum of squares was computed. For each experimental group, 1,000 reference data sets were generated via Monte-Carlo sampling from a uniform distribution over a box aligned with the principal components of the participants' data matrix. The *k*-means procedure was repeated for each reference data set. The optimal number of clusters was then chosen as the one for which the experimental within-cluster sum of squares differed most from its related null reference distribution. An optimal solution of 1 cluster would indicate the lack of separation of participants into distinct clusters.

Structural asymmetry. To assess group differences in structural hemispherical asymmetry, voxel-based morphometry of structural data in each separate data set was analyzed using FSL-VBM[54], an optimized VBM protocol[55] carried out with FSL tools[56]. First, segmented structural images in MNI-152 standard space were averaged and flipped along the *x*-axis to create a left-right–symmetric, data set–specific gray matter template. Second, all native gray matter images were nonlinearly registered to this data set–specific template and modulated to correct for local expansion (or contraction) due to the nonlinear component of the spatial transformation. The modulated gray matter images were then smoothed with a range of isotropic Gaussian kernels with σ value of 2–4 mm. Each participant's image was then flipped along the *x* axis, and a laterality map was created by computing the voxel-wise difference between the original and flipped images, divided by their sum (higher absolute values representing more laterality). The average of the absolute voxel values of each participant was derived, and the ratios between ASD and control group means were assessed for consistency across data sets.

Correlation with behavioral measures. The level of distortion in interhemispheric connectivity patterns was next measured. Specifically, the control mean interhemispheric connectivity voxel values across data sets were subtracted from each ASD participant's voxel values. This resulted in a map of differences for each participant with ASD. The variance of differences across voxels (distortion index) was calculated for each participant, and correlated with the participants' ages, IQ scores, ADI-R scores and ADOS-G scores (for participants with available clinical scores).

The significance of correlations was tested using a randomization test. For each clinical or demographical measure separately, the null distribution, assuming no correlation between this measure and the distortion index, was constructed by randomly shuffling the participants' distortion indices and correlating these with the unshuffled clinical or demographical measures. These values were used as previously described, and *P* values were Bonferroni-corrected to account for multiple comparisons.

Distortion indices were also calculated for control participants. To establish complete independence between single-subject data and group data, the control group voxel values subtracted from each control participant's voxel values were created without including that particular participant, and the variance of differences for that participant was then calculated. Group differences in interhemispheric connectivity spatial distortions were tested using a randomization test, as previously described, under the null hypothesis of no difference in distortion indices between experimental groups.

Intrahemispheric connectivity and heterotopic interhemispheric connectivity. For each hemisphere separately, single-subject time courses of gray-matter voxels that are mutual to the ASD and control participants of each separate data set were extracted. By cross-correlating these time courses within each participant, single-subject cross-correlation matrices were created for each hemisphere. These matrices are the equivalent of using each voxel as seed for an intrahemispheric functional connectivity analysis, and they thus reflect a high-resolution measure of intrahemispheric connectivity patterns. To test whether there was a global reduction in intrahemispheric connectivity in the ASD groups as compared to the control groups, the mean lower triangular value of each single-subject cross-correlation matrix was calculated for each hemisphere. For each data set and hemisphere, these single-subject values were averaged separately within the control and ASD groups, and the ratios between ASD and control group means were calculated. The uniformity of directionalities was assessed in each of the two resulting sets of ratios (created for each hemisphere across the five data sets).

Next, group differences in inter-subject spatial correlation of intrahemispheric connectivity patterns were examined. Specifically, for each data set separately and for each hemisphere separately, spatial correlations were computed between the lower triangular cross-correlation matrix of each participant and those of each other participant of the same experimental group. This procedure yielded two similarity matrices (one for each hemisphere) for each experimental group in each data set. Lower triangular values of each similarity matrix were then averaged, and the ratio between ASD and control averaged values were derived for each data set and hemisphere. The uniformity of directionalities across each set of five hemisphere-specific ratios was assessed. Effect magnitudes were determined using randomization tests and tested using the same statistical procedure as described above.

Within-hemisphere single-subject distortion indices were computed for each hemisphere separately by subtracting the mean control matrix values from the corresponding matrix values of each participant with ASD and calculating the variance of differences. The two resulting distortion indices for each participant (one for each hemisphere) were correlated with ASD symptoms, age and IQ measures. Correlations were submitted to the same statistical procedure as described for the homotopic interhemispheric connectivity case.

Heterotopic interhemispheric cross-correlation matrices were also created by cross-correlating time courses of the right hemispheres with those of the left hemisphere in each participant. The same procedures described above (global functional connectivity, inter-subject spatial correlation, distortion index) were carried out for all values comprising these single-subject matrices.

Intrahemisphere connectivity as a function of distance. For each hemisphere and data set separately, the coordinates of common gray-matter voxels of the two experimental groups were extracted, and the Euclidean distance between each pair of voxels in MNI space was calculated. Voxel-distance thresholds of 3 cm, 6 cm, 9 cm and 12 cm were applied to the intrahemispheric cross-correlation matrices of each participant, and the global connectivity and inter-subject spatial correlation analyses were repeated for each subset of connections, as described above. Note that each subset of resulting connections covered voxels of the entire hemisphere, as relevant connections were chosen for each voxel.

Control analyses. *Head movements.* To ensure that no bias was introduced by the scrubbing procedure, the number of time points was compared between data of participants from the two experimental groups in each separate data set using a randomization test, under the null hypothesis of no group difference in the number of scrubbed time points. To examine residual group difference in head movements, the variability of head motion was calculated for each of the six motion axes for each participant within the corresponding temporal mask. The motion variability in each axis was then compared between experimental groups of each separate data set using a randomization test, under the null hypothesis of no group difference in motion variance.

Brain alignment. To evaluate group differences in the extent of data distortion caused by the transformation to standard space, the Jacobian determinants of the deformation fields were compared between groups. Specifically, both the single-subject average and variance of Jacobian determinants across voxels were compared between experimental groups of each data set separately using a randomization test, under the null hypothesis of no group difference in either Jacobian mean or Jacobian variance.

IQ. To ensure that differences in IQ were not related to differences in inter-subject spatial correlations, the inter-subject FSIQ differences were calculated and correlated with the corresponding inter-subject similarity values, for each experimental group and type of connections. Corresponding *P* values were calculated using permutation tests, as described above.

Mathematical formulation of analysis pipeline. *Connectivity types.* Connectivity was computed using the Pearson correlation coefficient r^v between two voxel time courses, $\vec{v}_i$ and $\vec{v}_j$. We used three different types of $\vec{v}_i, \vec{v}_j$ connectivity:

Homotopic interhemispheric connectivity. This used time courses of each pair of two homologous voxels $v_i = (x,y,z), v_j = (-x,y,z)$.

Heterotopic interhemispheric connectivity. This used time courses of each and every voxel v_i in one hemisphere and each and every voxel v_j in the second hemisphere.

Intrahemispheric connectivity. This used time courses of each and every voxel v_i in one hemisphere and each and every voxel v_j in the same hemisphere.

Data set–specific analyses and their integration across data sets. For each data set $k = 1..5$, the ratio R between the statistic of the ASD group ($T^{k,A}$) and the statistic of the control group ($T^{k,C}$) was computed:

$$R_k = \frac{T^{(k,A)}}{T^{(k,C)}}$$

For a full list of statistics, see below.

We are interested in the consistency of effect directionalities across data sets. That will be established with high degree of certainty ($P < 0.05$) provided that lower statistic values in ASD groups satisfy $R_k < 1$ for each $k = 1..5$.

In cases where the requirement for consistency of effect directionalities was satisfied, data set–specific effect magnitudes were assessed using randomization tests, and *P* values were derived. The magnitude of consistency was tested, for example, using Fisher's method, using the data set–specific *P* values:

$$x^2_{2k} = -2\sum_{i=1}^{k}\ln(p_i)$$

List of statistics. Each of the below statistics were calculated for each data set ($k = 1..5$) and each experimental group (A/C).

Group-level 'regression to the mean' effect. The test statistic was defined as the cross-voxel variance of $\vec{M}$, an array of voxel values representing group-wise interhemispheric connectivity:

$$T^{k,A/C} = S^2\left(\vec{M}^{k,A/C}\right) = \frac{\sum_{i=1}^{N}\left(\vec{M}_i^{k,A/C} - \frac{1}{N}\sum_i^N \vec{M}_i^{k,A/C}\right)^2}{N}$$

where *N* signifies the number of voxels in the array.

Single-subject 'regression to the mean' effect. Cross-voxel variance of the homotopic interhemispheric connectivity voxel array was calculated for each participant. The test statistic was defined as the average of these variances across participants:

$$T^{(k,A/C)} = \frac{1}{n}\sum_{i=1}^{n} S^2(\vec{m}_i^{k,A/C})$$

where *n* signifies the number of participants of an experimental group and $\vec{m}_i^{k,A/C}$ signifies an array of voxel values of a single participant in a given data set and experimental group.

doi:10.1038/nn.3919

Global connectivity. The average of connectivity values (types described above) was calculated for each participant. The test's statistic was derived by averaging these values across participants in each data set and experimental group separately:

$$T^{k,\mathrm{A/C}} = \frac{\sum_{i,j}^{n,m} r_{i,j}^{v:k,\mathrm{A/C}}}{nm}$$

where n signifies the number of participants of an experimental group, m signifies the length of the correlation array and $r_{i,j}^{v:k,\mathrm{A/C}}$ signifies a correlation value between two voxel time courses, which is at position j in the correlation array of a given participant i in data set k and experimental group A or C.

Inter-subject spatial correlation. The lower triangular element of a similarity matrix was derived by computing the correlation coefficient r^s between the connectivity values of each participant and the corresponding values of each other participant of the same experimental group and data set. The test's statistic was defined as the average of these values across participants:

$$T^{k,\mathrm{A/C}} = \frac{2}{n(n-1)} \sum_{i=1}^{\frac{n(n-1)}{2}} r_i^{s:k,\mathrm{A/C}}$$

where n signifies the number of participants in a given experimental group and

$$\frac{n(n-1)}{2}$$

is the number of entries of the lower triangular element of a similarity matrix.

A **Supplementary Methods Checklist** is available.

37. Jenkinson, M., Bannister, P., Brady, M. & Smith, S. Improved optimization for the robust and accurate linear registration and motion correction of brain images. *Neuroimage* **17**, 825–841 (2002).
38. Smith, S.M. Fast robust automated brain extraction. *Hum. Brain Mapp.* **17**, 143–155 (2002).
39. Greve, D.N. & Fischl, B. Accurate and robust brain image alignment using boundary-based registration. *Neuroimage* **48**, 63–72 (2009).
40. Zhang, Y., Brady, M. & Smith, S. Segmentation of brain MR images through a hidden Markov random field model and the expectation-maximization algorithm. *IEEE Trans. Med. Imaging* **20**, 45–57 (2001).
41. Power, J.D., Barnes, K.A., Snyder, A.Z., Schlaggar, B.L. & Petersen, S.E. Spurious but systematic correlations in functional connectivity MRI networks arise from subject motion. *Neuroimage* **59**, 2142–2154 (2012).
42. Hallquist, M.N., Hwang, K. & Luna, B. The nuisance of nuisance regression: spectral misspecification in a common approach to resting-state fMRI preprocessing reintroduces noise and obscures functional connectivity. *Neuroimage* **82**, 208–225 (2013).
43. Fox, M.D., Zhang, D., Snyder, A.Z. & Raichle, M.E. The global signal and observed anticorrelated resting state brain networks. *J. Neurophysiol.* **101**, 3270–3283 (2009).
44. Hahamy, A. *et al.* Save the global: global signal connectivity as a tool for studying clinical populations with functional magnetic resonance imaging. *Brain Connect.* **4**, 395–403 (2014).
45. Saad, Z.S. *et al.* Trouble at rest: how correlation patterns and group differences become distorted after global signal regression. *Brain Connect.* **2**, 25–32 (2012).
46. Fisher, R.A. *Statistical Methods for Research Workers* (Genesis Publishing, 1925).
47. Fisher, R. Questions and answers #14. *Am. Stat.* **2**, 30–31 (1948).
48. Stouffer, S.A., Suchman, E.A., DeVinney, L.C., Star, S.A. & Williams, R.M. Jr. *The American Soldier, Vol. 1: Adjustment during Army Life* (Princeton Univ. Press, 1949).
49. Liptak, T. On the combination of independent tests. *Magyar Tud. Akad. Mat. Kutato Int. Kozl.* **3**, 171–197 (1958).
50. Glover, G.H. *et al.* Function biomedical informatics research network recommendations for prospective multicenter functional MRI studies. *J. Magn. Reson. Imaging* **36**, 39–54 (2012).
51. Hedges, L.V. & Olkin, I. *Statistical Methods for Meta-analysis* (Academic, Boston and London, 1985).
52. Turner, H.M. & Bernard, R.M. Calculating and synthesizing effect sizes. *Contemp. Issues Commun. Sci. Disord.* **33**, 42–45 (2006).
53. Hentschke, H. & Stüttgen, M.C. Computation of measures of effect size for neuroscience data sets. *Eur. J. Neurosci.* **34**, 1887–1894 (2011).
54. Douaud, G. *et al.* Anatomically related grey and white matter abnormalities in adolescent-onset schizophrenia. *Brain* **130**, 2375–2386 (2007).
55. Good, C.D. *et al.* A voxel-based morphometric study of ageing in 465 normal adult human brains. *NeuroImage* **14**, 21–36 (2001).
56. Smith, S.M. *et al.* Advances in functional and structural MR image analysis and implementation as FSL. *NeuroImage* **23** (suppl. 1): S208–S219 (2004).